ACS OMEGA

http://pubs.acs.org/journal/acsodf

Article

Inspecting Histamine Isolated from Fish through a Highly Selective Molecularly Imprinted Electrochemical Sensor Approach

Muhammad Abdurrahman Munir,* Fitria Rahmawati,* Jamia Azdina Jamal, Sofian Ibrahim, Mazlina Mohd Said, and Mohamad Syahrizal Ahmad

Cite This: *ACS Omega* 2023, 8, 13352−13361

Read Online

ACCESS | Metrics & More | Article Recommendations

ABSTRACT: Numerous analytical approaches have been developed to determine histamine levels in food samples due to its health consequences. Consuming histamine over the Food and Drug Administration (FDA)-regulated 50 mg kg^{-1} limit would result in chronic toxicity. Consequently, the present study discusses a novel electrochemical approach to evaluate histamine levels in fish products via a molecularly imprinted polymer (MIP) on an electrode surface. The film was produced with electropolymerized polyurethane (PU), which maintained the histamine compound. Fourier-transform infrared (FTIR) spectroscopy was applied to verify the MIP manufactured in this study. The capability of the polymer was measured by assessing its electron shifts with cyclic voltammetry (CV) and electrochemical impedance spectroscopy (EIS). Differential pulse voltammetry (DPV) was also employed to validate the sensing method. The MIP/screen-printed electrode (SPE) and non-imprinted polymer (NIP)/SPE recorded a linear response ranging from 1 to 1000 nmol L^{-1} at the 1.765 and 709 nmol L^{-1} detection limits. The sensing technique was subsequently utilized to determine the histamine levels in selected samples at room temperature (25 °C). Generally, the sensor allowed the accurate and precise detection of histamine in the fish samples. Furthermore, the approach could be categorized as a simple technique that is low-cost and suitable for on-site detections.

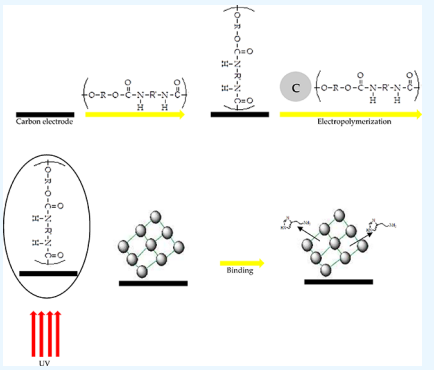

1. INTRODUCTION

Food safety has become a pressing issue that must be appropriately handled, given that food could be contaminated easily.[1] The World Health Organization (WHO) reported on 2000−2020 that one in 10 people suffers from food poisoning, while almost half of a million have died from food poisoning.[2] In Southeast Asia, particularly in Indonesia and Malaysia, food poisoning has resulted in 22.8 million cases of diarrhea and 37,600 thousand fatalities. Consequently, food security and monitoring are imperative.[3]

Aquatic foods have been most related to security issues considering the massive consumption of aquatic food products in Southeast Asia.[4] Physicochemical reactions in food commonly occur during storage. The reactions are influenced by several factors, such as heat, light, packaging process, and moisture. Furthermore, food adulteration might alter food content, which might lead to health threats.[5]

Aquatic food products offer high nutritional values that benefit humans. Nonetheless, aquatic nourishments contain high oil and fat levels compared to land-dwelling animals, which could lead to obesity, diabetes, and cardiovascular problems.[6] Consequently, nutrition experts suggested fish as the best choice as it is low in fat and rich in protein. Moreover, fish consumption serves various merits to the human body.[7]

Decarboxylation turns fish muscles into biogenic amines, which is a concern. Histamine is the most popular biogenic amine and thus has been the attention of numerous researchers. The presence of histamine in the bloodstream could result in several adverse effects, including histamine poisoning, a type of food toxicity. The symptoms of histamine poisoning range from mild to moderate to high risk and are even life-threatening.[8]

Food poisoning from histamine is commonly related to several aquatic animals, including sardines, mackerels, tunas, anchovies, and herrings. Accordingly, several countries have regulated the consumption of histamine-containing fish. For example, the Food and Drug Administration (FDA) in the United States of America (USA) only allowed 50 mg kg^{-1} of histamine intake, whereas a limit of 100−200 mg kg^{-1} has been set by the European Union (EU).[9] Consequently, developing a

Received: February 6, 2023
Accepted: March 20, 2023
Published: March 29, 2023

cost-effective and fast technique for histamine detection is critical.[10]

Various methods have been employed to analyze histamine levels in food, where most are chromatography-based. Nevertheless, the techniques require long analysis periods, complex instruments, and derivatizing agents to procure histamine and increase the sensitivity of high-performance liquid chromatography (HPLC).[11,12] Moreover, applying gas chromatography (GC) is restricted to laboratory facilities. The technique also involves complex preprocessing methods and typically requires a derivatization process, which is unsuitable for daily and on-site histamine detections.[13] Enzyme-linked immunosorbent assay (ELISA) offers a specific technique for determining histamine levels. Nonetheless, the approach necessitates a specific environment to maintain its detection sensitivity and stability.[14]

Compared to conventional methods, colorimetric is a better choice for histamine detection regarding its simplicity and rapidity, attracting the attention of scientists.[15] Nevertheless, the approach has limitations, such as low accuracy, insufficient extinction coefficient, and low color resolution, which leads to estimation inaccuracies. Consequently, applying biosensors in histamine detection offers an alternative that combines a bio-receptor and a transduction scheme.[16]

Biosensors provide several advantages, including rapid response, low cost, ease of operation, and high selectivity and accuracy.[17] Commonly, biosensors employ antibodies or enzyme materials as bio-receptors due to their satisfactory selectivity.[18] Nonetheless, they are also costly and possess low stability caused by several factors, such as temperature, humidity, ionic content, and pH.[19]

Specific substances, such as molecularly imprinted material (MIP) utilized as a recognition material solution, offer several superiorities, including high accuracy and sensitivity, fast analysis, and on-site applicability.[20] The MIP is a synthetic material produced by cross-linking monomers with polymerizing functions.[21] The substance also provides satisfactory stability, ease of production, cost-effectiveness, and robustness.[22]

The electrical parameters of building electrochemical sensor electrode surfaces require specific regulations that necessitate fulfillment to obtain satisfactory and reproducible materials and, hence, an adequate sensing instrument. Nevertheless, the process would not be straightforward if the analytes are oxidized below their potential values, particularly histamine.[23]

Currently, several MIP materials are available for detecting histamine.[24] Nonetheless, only few studies have reported the manufacture of MIP through electropolymerization.[25,26] The present study is the first to combine MIP with electropolymerized polyurethane (PU), producing an electrochemical sensor for on-site histamine assessments.

The PU is a unique polymer with several advantages, including good stability, ease of production, low cost, and good electrical properties, thus making it applicable for histamine detections that utilize electrochemical sensors.[27] The MIP film in this study was acquired by choosing the best parameters to develop a PU-based imprinted film. The electrochemical sensor was also validated, verified, and subsequently employed to analyze histamine in selected samples.

2. MATERIALS AND METHODS

2.1. Instruments. The electrochemical assessments in the current study were performed on a Metrohm Autolab Electrochemical Workstation provided by the Faculty of Science and Technology, Universiti Kebangsaan Malaysia (UKM). The screen-printed electrode (SPE), designed by Nurlely et al.,[28] was obtained by dropping argentum chloride (AgCl) and argentum (Ag) inks printed on the surface of a plastic sheet manufactured by Scrint Technology, Malaysia, and UKM. The SPE consisted of a 12.57 mm^2 active surface area and a 4 mm electrode diameter. In this study, the SPE was employed as the working electrode, while Ag/AgCl with a double-junction system and platinum wire were the reference and auxiliary electrodes, respectively.

2.2. Reagents. All reagents were applied in this study without purification. The current study also employed histamine (≥99%) purchased from Sigma Aldrich Sdn. Bhd. Potassium hexacyanoferrate III ($K_3[Fe(CN_6]$) and potassium hexacyanoferrate II-3-hydrate ($K_4[Fe(CN_6]\ 3H_2O$) were obtained from Merch Sdn. Bhd., sulfuric acid (H_2SO_4) (≥97%) and lithium perchlorate were purchased from Sigma Aldrich, and PU was produced according to the procedure outlined by Munir et al.[27] The present study acquired phosphate buffer solution (PBS) by mixing sodium dihydrogen phosphate ($Na_2H_2PO_4$) and disodium hydrogen phosphate (Na_2HPO_4), which were both purchased from Merck, Sdn. Bhd. This study also utilized ultrapure Milli-Q water.

2.3. Histamine Isolation from Fish. The fish employed in the present study was *Rastrelliger kanagurta*, a mackerel. The fish was selected to determine the accuracy and precision of the sensor manufactured in this study. The fish was bought from a local market. The fish was stored in a 4 °C fridge for 1 day. In the first step of UAI, approximately 2 g of the fish sample was dissolved in 10 mL of 2.5% trichloroacetic acid (TCA) and homogenized with a centrifuge. Subsequently, the homogenized samples were transferred into a 20 mL centrifuge tube before adding another 10 mL of 2.5% TCA to degrade the proteins.

The centrifuge tubes were placed in an ultrasonicator for 5 min at 50 °C to conduct the ultrasound-assisted isolation (UAI) method. The tubes were then cooled and centrifuged for 5 min at 2000 rpm. Finally, the mixture was filtered with a 0.45 μm membrane filter and diluted in PBS (100 mmol L^{-1}) before being analyzed with an electrochemical sensor, whereas the detection using chromatography approaches has been studied and published by Munir et al.[4]

2.4. Solutions. All solutions employed in this study were prepared with ultrapure water and stored at 4 °C. The SPE was cleansed with H_2SO_4 (0.1 M). The histamine (100 nmol L^{-1}) and PU (0.01 M) were combined with lithium perchlorate (0.1 M) to produce the MIP film that would be subjected to the polymerization mixture. A control sample, or a non-imprinted polymer (NIP), was obtained with PU (0.01 M) in lithium perchlorate (0.1 M).

In this study, the behavior of histamine (100 nmol L^{-1}) and a combination of cadaverine, putrescine, and histamine in a similar concentration (100 nmol L^{-1}) was applied to assess the sensitivity and selectivity of the established technique. The calibration curves of standard histamine solutions in lithium perchlorate (0.1 M) within the 1−1000 nmol L^{-1} range were also obtained. The $[Fe(CN)_6]^{4-}$ and $[Fe(CN)_6]^{3-}$ solutions of 10 mM each were also incorporated into PBS (100 mmol L^{-1}) to establish their electrical changes.

2.5. Screen-Printed Electrode Preparation. The SPE, which the current study employed as the working electrode, was cleansed via electrochemical treatment with cyclic

https://doi.org/10.1021/acsomega.3c00768
ACS Omega 2023, 8, 13352−13361

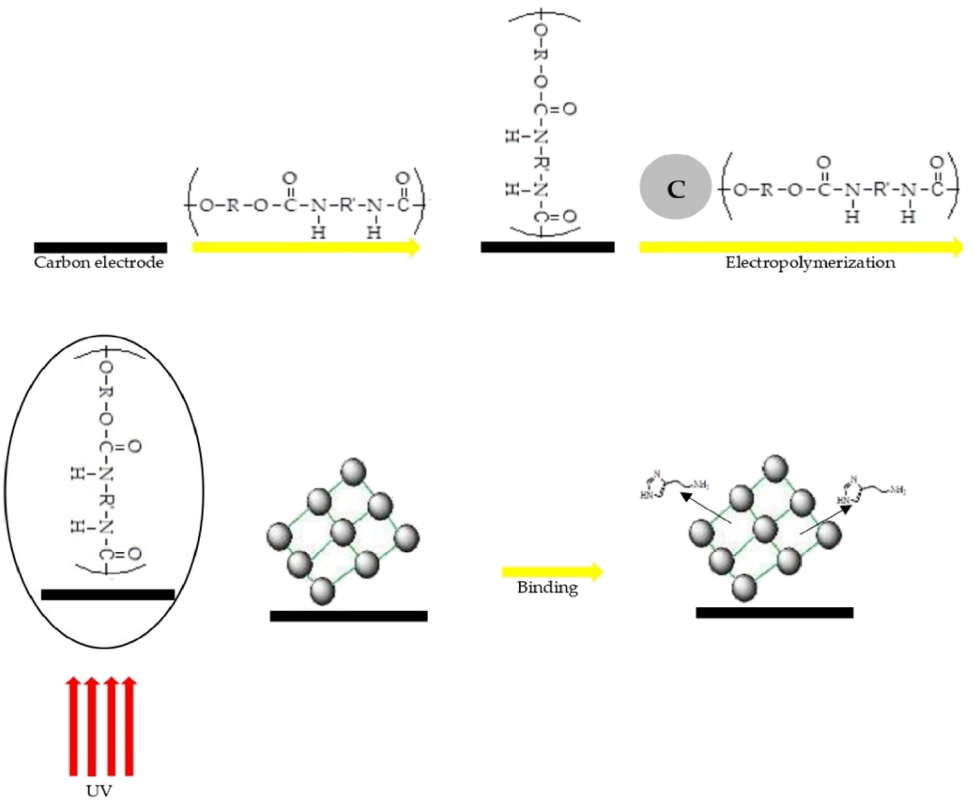

Figure 1. MIP sensor for histamine detection fabrication schematic illustration.

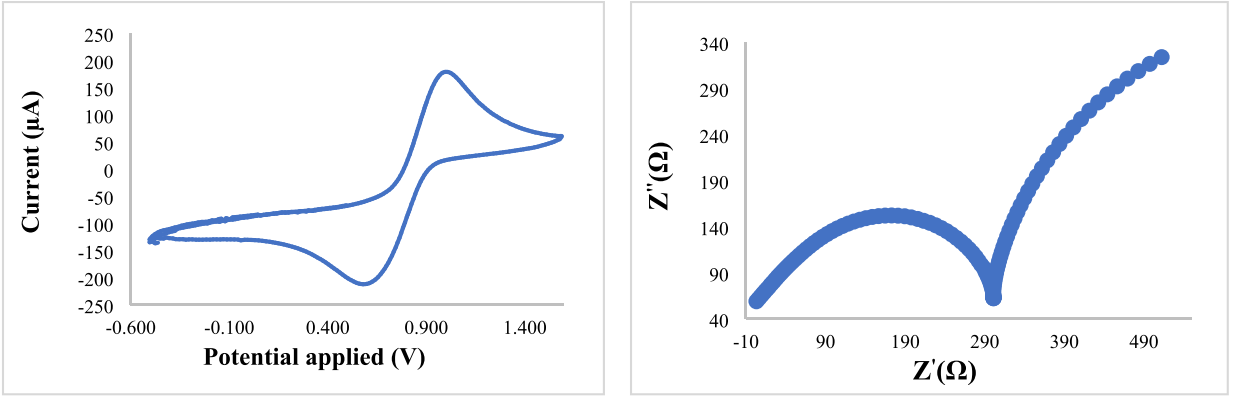

Figure 2. (a) CV and (b) EIS of the unmodified screen-printed electrode in PBS (100 mmol L^{-1}).

voltammetry (CV) within the −0.1 to +1 range at 1.5 and 0.05 V scan rates and in 10 cycles in H_2SO_4 (0.1 M). Subsequently, ultrapure water was applied to clean the SPE surfaces.

The polymerization mixture and chronoamperometry technique were applied at +0.70 V for 100 s to produce the MIP. During the step, a metal-free photo atom transfer radical polymerization (ATRP) grafting step was produced by employing a pulsed UV laser as a light source to manufacture a thin MIP film on the electrode surface.[29] Last, the template was expunged by incubating the film with ultrapure water (see Figure 1).

2.6. FTIR Analysis. The FTIR analysis in the present study was conducted with a PerkinElmer Spectrum BX with a diamond attenuation total reflectance (DATR) approach to verify the MIP and NIP structures, respectively. The assessment was performed at 4000−600 cm^{-1} to verify the essential peaks.[30]

2.7. MIP Morphological Analysis. The morphological characteristics of the MIP and NIP films manufactured in this study were evaluated with a field emission scanning electron microscope (FESEM) (Gemini SEM microscope model 500-7022). Before the assessment, the polymer was coated with a thin layer of gold to enhance its conductivity by utilizing a sputter-coater. The inspections were performed at 200 and 5000× magnifications and 10.00 kV electron high tension (EHT).

2.8. Electrochemical Procedures. The electrochemical measurements performed during this study were in six replicates. The CV scanned potentials from −0.5 to +0.5 V at 0.05 V s^{-1}, which provided electrochemical reaction rates

https://doi.org/10.1021/acsomega.3c00768
ACS Omega 2023, 8, 13352−13361

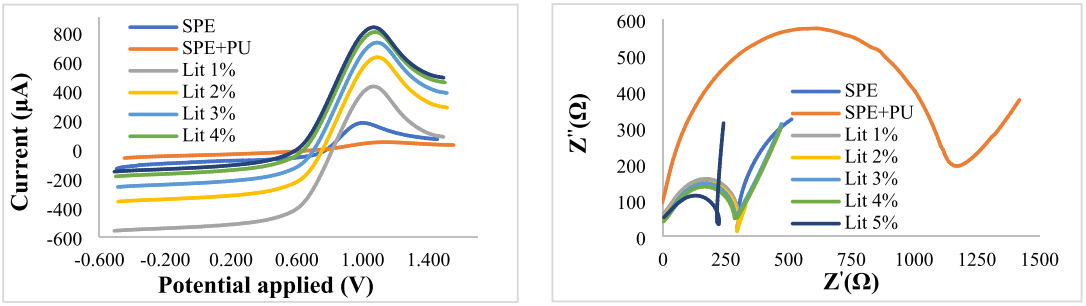

Figure 3. (a) CV and (b) EIS of unmodified and modified SPE with various concentrations of lithium perchlorate in PBS (100 mmol L^{-1}).

and redox potential as the outcomes. The EIS was applied in the present study to determine the conductivity of the MIP obtained. The evaluation parameters were a sinusoidal wave (0.01 V, amplitude) at an open circuit potential and 100 data points within the 0.1−100000 Hz frequency range and logarithmically distributed.

The EIS results were employed to establish the Randles equivalent circuit and Nyquist plots. The conditions applied reflected the kinetic reactions on the electrolyte−electrode interface. The interface or the specific sections of the impedance was addressed as resistance or Z', and the imaginary part or Z''. Furthermore, the Nyquist plot recorded a semi-circle that could be utilized in charge-transfer resistance (R_{ct}) estimations.[40] In this study, differential pulse voltammetry (DPV) was also conducted due to it is selectivity and sensitivity over CV.[31] The scanning potentials employed during the DPV ranged from −0.1 to +0.9 V.

The redox probe solution response was obtained after alterations had occurred at the sensing surface electrode linked to electrical properties. The detection limit (DL) was acquired from the linear response with the formula $x + 3\sigma$, where x is the mean value of the blanks and σ is the standard deviation. Since other biogenic amines are also commonly discovered in fish products, biogenic amines, such as cadaverine and putrescine, were also utilized to determine the selectivity and sensitivity of the approach. Similar concentrations of histamine, cadaverine, and putrescine were employed (100 nmol L^{-1}). Furthermore, two approaches such as MIP/SPE and NIP/SPE were employed to detect the histamine and mixed biogenic amine solutions.

3. RESULTS AND DISCUSSION

3.1. Handling the SPE before Utilization. Cleaning the SPE before employment is crucial to avoid interferences during analysis. Accordingly, several cleaning techniques were performed in this study to ascertain the reproducibility of the sensors procured. The present study utilized 98% ethanol to cleanse the electrode surfaces thrice. The electrode surfaces were also purified thrice with 98% ethanol before cleaning the CV with H_2SO_4 (0.1 N) solution. Another step was employing only the CV with H_2SO_4 (0.1 N) during cleaning. Resultantly, the ideal cleaning parameters were 10 cycles of −0.1 to 1.5 V potential. The CV and EIS plots acquired under the optimal parameters are presented in Figure 2.

The SPE in the current study was purified and modified to produce an amine layer on its surface, thus generating the MIP. The MIP film was stably attached to the SPE surface, although the PU electropolymerization influenced the amine layer

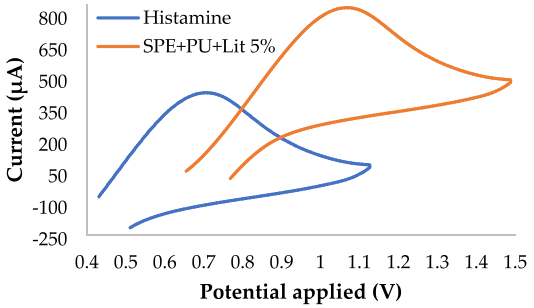

Figure 4. Cyclic voltammograms of the modified electrode without histamine (SPE + PU + Lit 5%) and modified electrode containing histamine in detecting the potential applied of histamine in 100 mmol L^{-1} PBS.

production through its aromatic groups.[32] Lithium perchlorate was also incorporated at various concentrations (1, 2, 3, 4, and 5%), which increased the conductivity of the PU and R_{ct}, as expected (see Figure 3).

3.2. Polymerization Application of Electrochemical Parameters. Electropolymerization refers to producing radical species from polymers to obtain MIP layers by employing particular electrical states on SPE surfaces. In this study, the histamine structure was made sure to be unaffected by the electrochemical conditions applied to avoid its involvement during polymerization on the SPE. If the histamine were affected, it would co-polymerize with PU and bind to the polymeric layer, limiting the number of binding sites formed.

The electrochemical characteristics of the PU and histamine (50 nmol L^{-1}) utilized in the present study were first examined in single and mingled solutions to avoid limitations. The evaluation ensured that the histamine and PU were electroactive in PBS (100 mmol L^{-1}) at identical potential ranges. Subsequently, other media were employed to verify the electrochemical condition where the histamine was inactive while the PU was active at an identical potential range.

The histamine solution was dissolved in PBS (100 mmol L^{-1}) and lithium perchlorate (0.1 M) during the electrochemical analysis by employing the electrode, NIP, and MIP. The outcomes are demonstrated in Figure 4. Lithium perchlorate application influenced the electroactivity of histamine, which was not detected at 0 to +0.6 V. Conversely, the electroactivity of PU persisted under similar parameters. The results indicated that the employment of lithium perchlorate as media permitted PU film formation without influencing the histamine structure on the electrode surface.

https://doi.org/10.1021/acsomega.3c00768
ACS Omega 2023, 8, 13352−13361

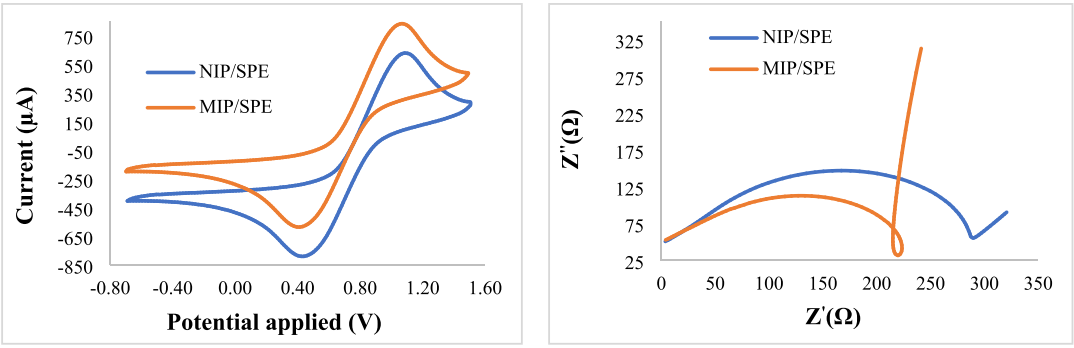

(a) (b)

Figure 5. (a) Cyclic voltammograms of NIP/SPE and MIP/SPE with lithium perchlorates (5%) in 100 mmol L^{-1} PBS and (b) EIS spectra of NIP/SPE and MIP/SPE in PBS (100 mmol L^{-1}).

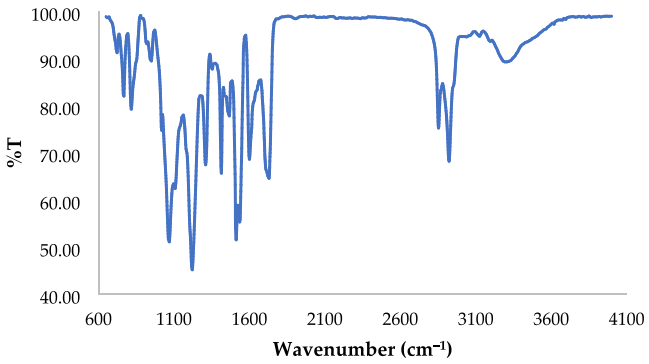

Figure 6. FTIR spectrum of the MIP film.

3.3. Sensing Coating Installation. In this study, electropolymerization was employed to produce the MIP film. The film was obtained through bulk polymerization with particular electrical parameters in a solution with histamine and PU as the template and polymer. The procedure also generated MIP for tiny-sized target analytes. The combination of electropolymerization and bulk polymerization was a practical technique considering the little reagent required. Moreover, the technique allowed imprinted areas to be attached to the outer layer of the electrochemical sensors as opposed to the surfaces.[23,33]

The formation of PU and histamine in the current study occurred in the pre-polymer arrangement owing to entangling hydrogen bond interactions. The polymeric system was subsequently shaped by radical reaction, which commenced after adequate potential to produce oxidized PU radicals was provided. Chronoamperometry was employed at +0.75 V for 100 s and validated.

A mixture of PU and histamine in lithium perchlorate was acquired via electropolymerization, which generated a film over the histamine. The NIP electrode, which was the control (blank), was obtained by employing the PU and lithium perchlorate, producing a film without histamine. The CV and EIS data are illustrated in Figure 5.

Generally, the anodic current reduction emphasized the polymeric reaction detected in CV (see Figure 5a). Moreover, compared to the SPE surface, the R_{ct} was increased in the Nyquist plot (see Figure 5b). The histamine in the MIP demonstrated a notable dissimilarity between the NIP and MIP electrodes due to the single experimental differences in the materials.

The SPE/MIP electrode CV measurements post chronoamperometry exhibited reduced anodic current and elevated peak separation compared to the SPE/NIP electrode (see Figure 5). Consequently, the presence of histamine in the polymeric network was confirmed by the high R_{ct} value in the MIP film. The altered electrical properties on the surface caused by the histamine also occurred when the polymer film grew. The

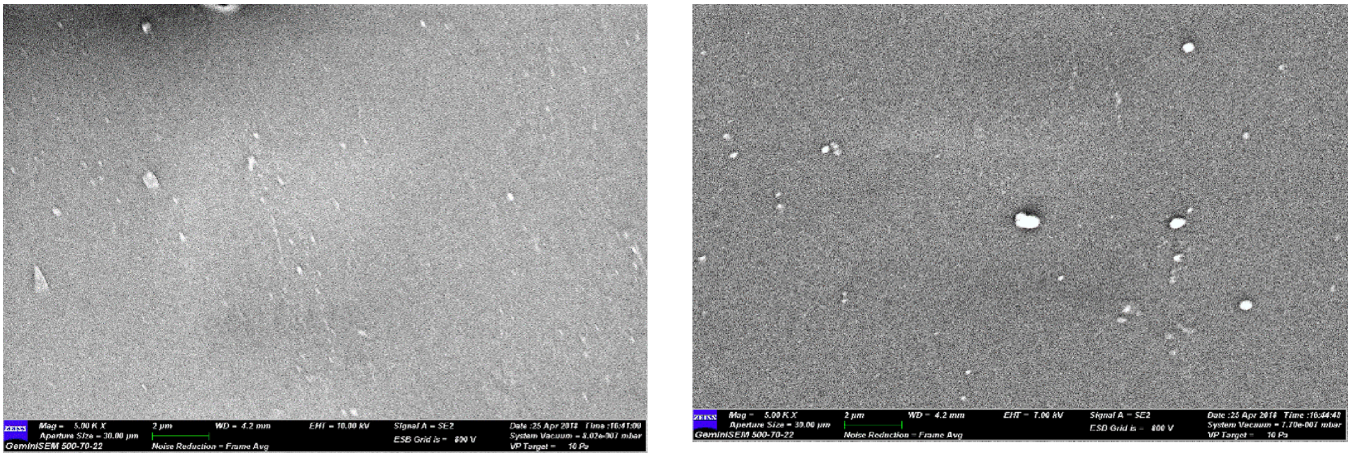

Figure 7. Micrograph of the MIP film observed through FESEM at 200−5000× magnifications.

https://doi.org/10.1021/acsomega.3c00768
ACS Omega 2023, 8, 13352−13361

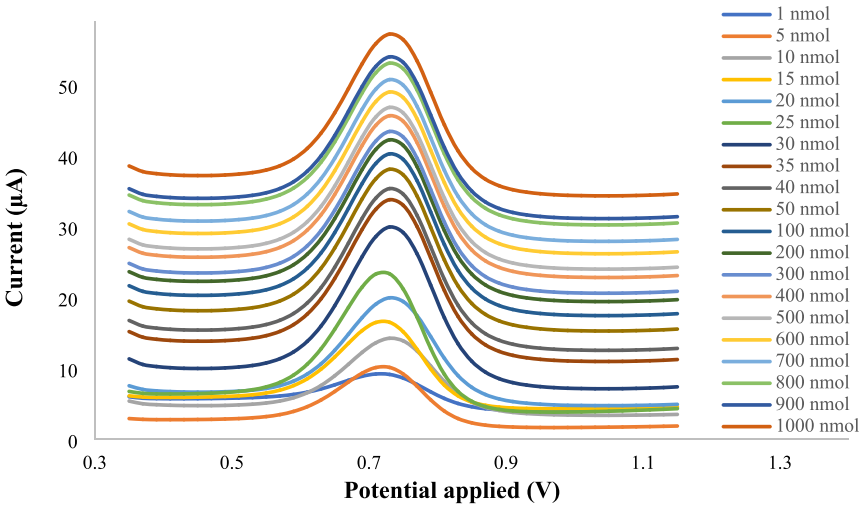

Figure 8. DPV voltammograms of histamine at various concentrations in PBS (100 mmol L^{-1}) at pH 7 on NIP/SPE/PU/$LiClO_4$.

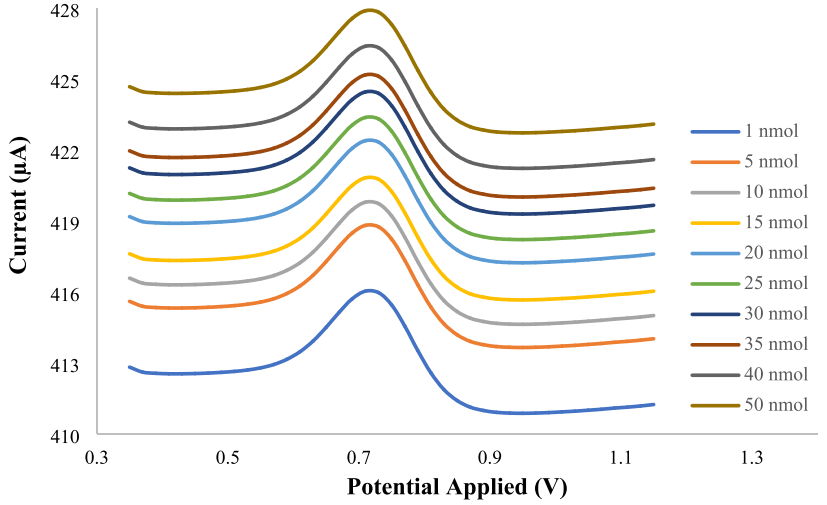

Figure 9. DPV voltammograms of histamine of varying concentrations in PBS (100 mmol L^{-1}) at pH 7 on MIP/SPE/PU/$LiClO_4$.

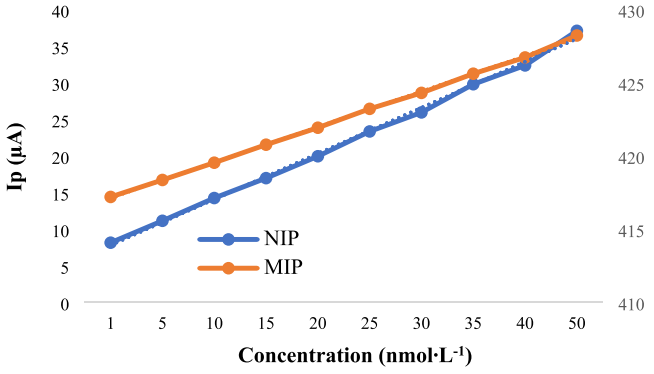

Figure 10. Voltage (μA) versus concentration (nmol L^{-1}) of the NIP/SPE/PU/$LiClO_4$ and MIP/SPE/PU/$LiClO_4$ calibration curves in different histamine concentrations (1−50 nmol L^{-1}).

observation indicated that histamine was not a conductive compound and that the PU possessed electrical features, mainly owing to the conductivity of PU related to its polymerization.[34]

In the first stage of MIP polymerization, the conductive polymer layer produced resulted in fewer radicals per unit of time production at the outer surface. The reproducibility of electrodes was also determined in this study. The CV and EIS analyses exhibited satisfactory reproducibility of the electrochemical approaches, taking into account the MIP and NIP electrode applications.

3.4. Histamine Purification from the Sensing Layer.

Disposing of histamine from the polymer network was a crucial and final step to completing the MIP installation. Histamine was removed to increase the number of binding sites to specific analytes that would be shaped inside the polymer during detection.[35] Water could dissolve histamine easily and was employed to dispose of histamine molecules from the MIP surfaces in the current study. The application of other solvents was evaded given their possible harm to the PU layer.

The MIP and NIP films were incubated in water, and the effectiveness of histamine removal from their surfaces by water was determined. The NIP and MIP film R_{ct} values escalated based on the Nyquist plot, while the CV anodic peaks were reduced. The results were due to the release of PU conductive oligomeric structures from the polymeric network.

Histamine recorded a positive charge with the applied parameters, thereby developing ionic interactions with the negatively charged iron redox probe. Histamine also donated

https://doi.org/10.1021/acsomega.3c00768
ACS Omega 2023, 8, 13352−13361

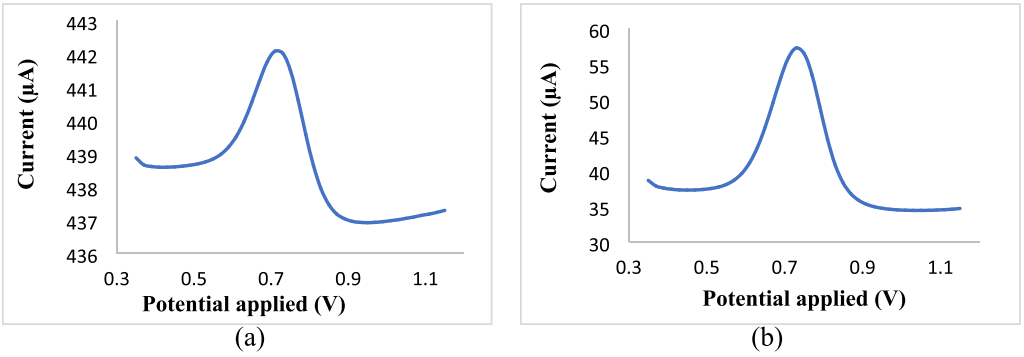

Figure 11. DPV voltammograms of histamine detected in the mackerel samples with PBS (100 mmol L^{-1}) at pH 7 on (a) MIP/SPE/PU/$LiClO_4$ and (b) NIP/SPE/PU/$LiClO_4$.

Table 1. Comparison of the Analytical Performance of Histamine Detection

parameters	Wang et al.[40]	Ahmed et al.[25]	Mahnashi et al.[41]	Fan et al.[42]	Peng et al.[43]	this study
technique	BELISA[a]	MIP-PANI/ PEDOT @ AuIO[b]	MIP-Au@Fe -BDC/N, S − GQDs/ GCE[c]	MISPE/ CE[d]	BELISA[a]	MIP/SPE/PU/ $LiClO_4$
linear range (mM)	8.99×10^{-5} to 8.99	5×10^{-5} - 5×10^{-1}	7.8×10^{-8} to 2.5×10^{-4}	0.89−899.68	8.9×10^{-6} to 8.99	1×10^{-6} to 5×10^{-5}
detection limit (mM)	6.2×10^{-4}	1×10^{-6}	2.6×10^{-8}	0.782	3.5×10^{-4}	1×10^{-7}
reproducibility (%)	1.7	1.9	1.8	1.8	5.35	0.98
stability (days)			49			60

[a]Biomimetic enzyme-linked immunoassay. [b]Molecularly imprinted polymer−polyaniline/3,4-ethylenedioxythiophene@gold inverse opal. [c]Metal organic framework/nitrogen−sulfur co-doped graphene quantum dots / glassy carbon electrode. [d]Molecularly imprinted solid-phase extraction−capillary electrophoresis.

an electron to modify the charge-transfer properties at the SPE surfaces. Generally, histamine disposal from the MIP and NIP film surfaces was effective. Furthermore, the PU film documented adequate stability when unwrapped from the water.

3.5. Electrochemical Sensor Characterization. The FTIR analysis was conducted in this study to verify the structure of the MIP and NIP films procured (see Figure 6). The MIP spectrum did not record the histamine structure, indicating that the histamine removal steps were complete and successful. Furthermore, the FESEM micrograph in Figure 7 demonstrates the formation of an MIP film post electropolymerization. The magnification applied to observe the MIP film surface was 200−5000×. Resultantly, electropolymerization ensured a successful MIP reaction, which was verified by the wavelengths in the FTIR spectra.

3.6. Analytical Approach Employing the Electrochemical Sensor. The determination of analyte depends on the sample treatment. The sample treatment is a crucial and fundamental step in ensuring that the desired analytes were isolated and interferences were expunged. Fish products are very complex and contain several major substances, such as fats, carbohydrates, proteins, and chemical additives. Accordingly, a specific technique to isolate analytes from samples with enhanced efficiency is critical.[36] The method should also be simple, sustainable, and rapid, require less solvent, and possess satisfactory disjunction capability.

Ultrasound is commonly applied for sample extractions due to its abilities during sample treatments. The approach necessitates only a little organic solvent to destroy the matrix that contains the desired analytes, thus accelerating and improving the isolation step. The UAI is commonly applied in analytical chemistry considering its swiftness, modesty, simplicity, and eco-friendliness.[37]

The present study performed DPV owing to its superior selectivity and sensitivity over CV. The method was conducted to determine the oxidation of histamine during analysis with NIP/SPE and MIP/SPE. Following various validation approaches to achieve the best scan rate, pulse time, and pulse amplitude, the optimized DPV conditions were 10 mV s^{-1} scan rate, 50 mV pulse amplitude, and 10 ms pulse time.

Varying histamine concentrations were analyzed via the DPV method post validation. Histamine analyses with the SPE/MIP and SPE/NIP electrodes involved adding the 100 nmol L^{-1} histamine standard to the SPE as a working electrode before being incubated for 15 min. The incubation was performed to ensure histamine attachment to the MIP and NIP films.

The histamine determination via DPV involved a three-electrode system and was replicated for several procedures. During the assessment, the histamine levels were escalated within the 1−1000 nmol L^{-1} range, and the NIP electrodes were also evaluated (see Figure 8). The SPE/MIP electrodes were employed to determine the blank solution and histamine levels within the 1−50 nmol L^{-1} range by utilizing lithium perchlorate to increase the voltage. A calibration curve, where x was histamine voltage and y was the values of potential applied, was also obtained (see Figure 9).

Figure 10 illustrates the NIP/SPE and MIP/SPE calibration curves. Based on the data, different histamine levels were detected in PBS (100 mmol L^{-1}) at pH 7. The NIP/SPE and MIP/SPE plots also enabled DL calculations with a specific equation containing the standard deviation of the intercept and the slope of the curves. The NIP/SPE DL was 709 nmol L^{-1}, whereas the MIP/SPE recorded 1.765 nmol L^{-1}.

https://doi.org/10.1021/acsomega.3c00768
ACS Omega 2023, 8, 13352−13361

The determination of histamine using MIP/SPE/PU/$LiClO_4$ using the voltammetric approach presents a satisfactory outcome. Generally, voltammetry relies on the development of current signal and charge upon histamine as the analyte and MIP as the receptor binder.[24] Various studies have reported several receptors such as enzymes and aptamers.[38,39]

The validated method was applied in determining the amount of histamine in the mackerel samples. The sample was analyzed in six replicates, and the voltammograms are demonstrated in Figure 11. The histamine standard was validated to obtain quantitative histamine levels in the fish. The MIP/SPE/PU/$LiClO_4$ detected 106.32 nmol L^{-1} histamine in the fish samples, while the NIP/SPE/PU/$LiClO_4$ recorded 81.49 nmol L^{-1}.

3.7. Comparison of the Current Validated Electrochemical Sensor with Other Reported Sensors for Determination of Histamine. The validated sensor via modification of MIP/SPE/PU/$LiClO_4$ in this study demonstrated improved performance in terms of, stability, response time, precision, and accuracy compared with other previously reported electrochemical sensors and biosensors for histamine detection listed in Table 1.

Among these studies mentioned in Table 1, the molecularly imprinted polymers (MIPs) are the most robust and stable, offering particular recognition properties that are suitable for on-site detection. The application of MIP offers a low detection limit, even though the detection limit of this study is higher than that of Mahnashi et al.;[41] in terms of stability, this method is better. Furthermore, the application of lithium perchlorate to increase the conductivity of SPE modification is cheaper compared to gold.

4. CONCLUSIONS

The present study successfully produced a histamine electrochemical sensor with MIP, resulting in a rapid, simple, easy-to-operate, and inexpensive method. The duration for histamine sensing was below 2 min, which was shorter than chromatography detection. Furthermore, solvent application during the electrochemical sensing provided in this study was very low, where only PBS was required. Conversely, in chromatography applications, several mobile phases are required. Obtaining the electroactivity of the target molecules was one of the challenges in this study. The issue was solved by applying experimental conditions that decreased histamine and maintained PU electroactivity. The receptor element was obtained in situ in a few seconds. Furthermore, on-site histamine detection in an aquatic environment could be performed very well. Nevertheless, a 15 min incubation must precede the procedure. The SPE/MIP instrument procured in the current study exhibited good histamine detection in terms of analytical performance and high selectivity and sensitivity compared to other biogenic amines, such as cadaverine and putrescine. Consequently, the instrument could be applied to determine the accumulation of biogenic amines that are often specifically detected in the food industry.

■ ASSOCIATED CONTENT

Data Availability Statement

Not applicable.

■ AUTHOR INFORMATION

Corresponding Authors

Muhammad Abdurrahman Munir − *Department of Pharmacy, Faculty of Health Sciences, Alma Ata University, 55184 Yogyakarta, Indonesia;* orcid.org/0000-0001-6129-6202; Email: muhammad@almaata.ac.id

Fitria Rahmawati − *Research Group of Solid State Chemistry and Catalysis, Chemistry Department, Faculty of Mathematics and Natural Sciences, Sebelas Maret University, 57126 Surakarta, Indonesia;* orcid.org/0000-0002-3145-9063; Email: fitria@mipa.uns.ac.id

Authors

Jamia Azdina Jamal − *Drug and Herbal Centre, Faculty of Pharmacy, Universiti Kebangsaan Malaysia, 50330 Kuala Lumpur, Malaysia*

Sofian Ibrahim − *Malaysian Nuclear Agency, 43000 Kajang, Bangi, Malaysia*

Mazlina Mohd Said − *Drug and Herbal Centre, Faculty of Pharmacy, Universiti Kebangsaan Malaysia, 50330 Kuala Lumpur, Malaysia*

Mohamad Syahrizal Ahmad − *Faculty of Science and Mathematics, Universiti Pendidikan Sultan Idris, 35900 Tanjung Malim, Malaysia*

Complete contact information is available at: https://pubs.acs.org/10.1021/acsomega.3c00768

Funding

This research was funded by Department of Pharmacy, Universiti Kebangsaan Malaysia, and the Article Processing Charge (APC) was funded by Sebelas Maret University, Indonesia.

Notes

The authors declare no competing financial interest.

■ ACKNOWLEDGMENTS

The authors extend their gratitude to the Program of World Class Professor (WCP) held by Direktorat Jenderal Pendidikan Tinggi, Kementerian Pendidikan dan Kebudayaan, Republic of Indonesia, for providing national funding. The authors would also like to thank UKM and the Malaysian Nuclear Agency for providing the materials and instruments. Appreciation is also extended to Sebelas Maret University for funding the publication fee.

■ REFERENCES

(1) Odeyemi, O. A. Public health implications of microbial food safety and foodborne diseases in developing countries. *Food Nutr. Res.* **2016**, *60*, 29819.

(2) World Health Organization (WHO) *Framework for action on food safety in the WHO South-East Asia region*; World Health Organization, Regional Office for South-East Asia: New Delhi.

(3) Gao, P.; Noor, N. Q. I. M.; Shaarani, S. M. Current status of food safety hazards and health risks connected with aquatic food products from Southeast Asian region. *Crit. Rev. Food Sci. Nutr.* **2020**, *13*, 3471−3489.

(4) Munir, M. A.; Mackeen, M. M. M.; Heng, L. Y.; Badri, K. H. Study of histamine detection using liquid chromatography and gas chromatography. *ASM Sci. J.* **2021**, *16*, 1−9.

(5) Cao, G.; Li, K.; Guo, J.; Lu, M.; Hong, Y.; Cai, Z. Mass spectrometry for analysis of changes during food storage and processing. *J. Agric. Food Chem.* **2020**, *26*, 6956−6966.

(6) Daschner, A. Risks and possible health effects of raw fish intake. *Fish Fish Oil Health Dis. Prev.* **2016**, 341−353.

(7) Krittanawong, C.; Isath, A.; Hahn, J.; Wang, Z.; Narasimhan, B.; Kaplin, S. L.; Jneid, H.; Virani, S. S.; Tang, W. Fish consumption and cardiovascular health: A systematic review. *Am. J. Med.* **2021**, *6*, 713−720.
(8) Kounnoun, A.; Maadoudi, M. E.; Cacciola, F.; Mondello, L.; Bougtaib, H.; Alahlah, N.; Amajoud, N.; EL Baaboua, A.; Louajri, A. Development and validation of a high-performance liquid chromatography method for the determination of histamine in fish samples using fluorescence detection with pre-column derivatization. *Chromatographia* **2020**, *83*, 893−901.
(9) Serrano, V. M.; Cardoso, A. R.; Diniz, M.; Sales, M. G.; Sales, G. F. *In-situ* production of histamine-imprinted polymeric materials for electrochemical monitoring of fish. *Sens. Actuators, B* **2020**, *311*, No. 127902.
(10) Munir, M. A.; Heng, L. Y.; Sage, E. E.; Mackeen, M. M. M.; Badri, K. H. Histamine detection in mackerel (*Scomberomorus* Sp.) and its products derivatized with 9-fluorenilmethylchloroformate. *Pak. J. Anal. Environ. Chem.* **2021**, *2*, 243−251.
(11) Zhou, T.; Fan, M.; You, R.; Lu, Y.; Huang, L.; Xu, Y.; Feng, S.; Wu, Y.; Shen, H.; Zhu, L. Fabrication of Fe_3O_4/Au@ATP@Ag nanorod sandwich structure for sensitive SERS quantitative detection of histamine. *Anal. Chim. Acta* **2020**, *1104*, 199−206.
(12) Munir, M. A.; Badri, K. H.; Heng, L. Y.; Inayatullah, A.; Nurinda, E.; Estiningsih, D.; Fatmawati, A.; Aprilia, V.; Syafitri, N. The application of polyurethane-$LiClO_4$ to modify screen-printed electrodes analyzing histamine in mackerel using a voltammetric approach. *ACS Omega* **2022**, *7*, 5982−5991.
(13) Inayatullah, A.; Badrul, H. A.; Munir, M. A. Fish analysis containing biogenic amines using gas chromatography flame ionization detector. *Sci. Technol. Indones.* **2021**, *1*, 1−7.
(14) Sontag, G.; Pinto, M. I.; Noronha, J. P.; Burrows, H. D. Analysis of food by high performance liquid chromatography coupled with coulometric detection and related techniques: A review. *J. Agric. Food Chem.* **2020**, *15*, 4113−4144.
(15) Huang, C.; Wang, S.; Zhao, W.; Zong, C.; Liang, A.; Zhang, Q.; Liu, X. Visual and photometric determination of histamine using unmodified gold nanoparticles. *Microchim. Acta* **2017**, *184*, 2249−2254.
(16) Wang, H.; Rao, H.; Luo, M.; Xue, X.; Xue, Z.; Lu, X. Noble metal nanoparticles growth-based colorimetric strategies: From monocolorimetric to multicolorimetric sensors. *Coord. Chem. Rev.* **2019**, *398*, No. 113003.
(17) Yu, X.; Zhong, T.; Zhang, Y.; Zhao, X.; Xiao, Y.; Wang, L.; Liu, X.; Zhang, X. Design, preparation and application of magnetic nanoparticles for food safety analysis: A review of recent advances. *J. Agric. Food Chem.* **2022**, *1*, 46−62.
(18) Krishnan, S. K.; Singh, E.; Singh, P.; Meyyappan, M.; Nalwa, H. S. A review on graphene-based nanocomposites for electrochemical and fluorescent biosensors. *RSC Adv.* **2019**, *9*, 8778−8881.
(19) Ahmed, I.; Lin, H.; Xu, L.; Li, S.; Costa, J.; Mafra, I.; Chen, G.; Gao, X.; Li, Z. Immunomodulatory effect of laccase/caffeic acid and transglutaminase in alleviating shrimp tropomyosin (Met e 1) allergenicity. *J. Agric. Food Chem.* **2020**, *29*, 7765−7778.
(20) Wang, H.; Huang, C.; Ma, S.; Bo, C.; Ou, J.; Gong, J. Recent advances of restricted access molecularly imprinted materials and their applications in food and biological samples analysis. *TrAC, Trends Anal. Chem.* **2022**, *147*, No. 116526.
(21) Song, Z.; Li, J.; Lu, W.; Li, B.; Yang, G.; Bi, Y.; Arabi, M.; Wang, X.; Ma, J.; Chen, L. Molecularly imprinted polymers based materials and their applications in chromatographic and electrophoretic separations. *TrAC, Trends Anal. Chem.* **2022**, *146*, No. 116504.
(22) He, S.; Zhang, L.; Bai, S.; Yang, H.; Cui, Z.; Zhang, X.; Li, Y. Advances of molecularly imprinted polymers (MIP) and the application in drug delivery. *Eur. Polym. J.* **2021**, *143*, No. 110179.
(23) Cardoso, A. R.; Tavares, A. P. M.; Sales, M. G. F. In-situ generated molecularly imprinted material for chloramphenicol electrochemical sensing in waters down to the nanomolar level. *Sens. Actuators, B* **2018**, *256*, 420−428.
(24) Venkatesh, S.; Yeung, C. C.; Li, T.; Lau, S. C.; Sun, Q. J.; Li, L. Y.; Li, J. H.; Lam, M. H. W.; Roy, V. A. L. Portable molecularly imprinted polymer-based platform for detection of histamine in aqueous solutions. *J. Hazard. Mater.* **2021**, *410*, No. 124609.
(25) Ahmed, S.; Ansari, A.; Haidyrah, A. S.; Chaudhary, A. A.; Imran, M.; Khan, A. Hierarchical molecularly imprinted inverse opal-based platforms for highly selective and sensitive determination of histamine. *ACS Appl. Polym. Mater.* **2022**, *4*, 2783−2793.
(26) Ibrahim, S.; Badri, K. H.; Ratnam, C. T.; Ali, N. H. M.; Munir, M. A. Radiation dose required for the vulcanization of natural rubber late via hybrid gamma radiation and peroxide vulcanizations. *IOP Conf. Ser.: Mater. Sci. Eng.* **2019**, *555*, No. 012026.
(27) Munir, M. A.; Badri, K. H.; Heng, L. Y.; Inayatullah, A.; Badrul, H. A.; Emelda, E.; Dwinta, E.; Kusumawardani, N.; Wulandari, A. S.; Aprilia, V.; Supriyono, R. B. Y. Design and synthesis of conducting polymer bio-based polyurethane produced from palm kernel oil. *Int. J. Polym. Sci.* **2022**, *2022*, 6815187.
(28) Nurlely, N.; Ahmad, M.; Heng, L. Y.; Tan, L. L. Potentiometric enzyme biosensor for rapid determination of formaldehyde based on succinimide-functionalized polyacrylate ion-selective membrane. *Measurement* **2021**, *175*, No. 109112.
(29) Ramakers, G.; Wackers, G.; Trouillet, V.; Welle, A.; Wagner, P.; Junkers, T. Laser-grafted molecularly imprinted polymers for the detection of histamine from organocatalyzed atom transfer radical polymerization. *Macromolecules* **2019**, *6*, 2304−2313.
(30) Asghari, A.; Hosseini, A. H.; Ghajarbeygi, P. Fast and non-destructive determination of histamine in tuna fish by ATR-FTIR spectroscopy combined with PLS calibration method. *Infrared Phys. Technol.* **2022**, *123*, No. 104093.
(31) Sahudin, M. A.; Tan, L. L.; Su'ait, M. S.; Karim, N. H. A.; Mackeen, M. M. M. Regenerable and selective histamine impedimetric sensor based on hydroxyl functionalised Schiff base complex electrode. *Electrochim. Acta* **2021**, *379*, No. 138186.
(32) Xu, S.; Wu, F.; Mu, F.; Dai, B. The preparation of Fe-based peroxidase mimetic nanozymes and for the electrochemical detection of histamine. *J. Electroanal. Chem.* **2022**, *908*, No. 116088.
(33) Chen, Z.; Zhang, Q.; Shan, J.; Lu, Y.; Liu, Q. Detection of bitter taste molecules based on odorant-binding protein-modified screen-printed electrodes. *ACS Omega* **2020**, *42*, 27536−27545.
(34) Kobayashi, Y.; Nakamitsu, Y.; Zheng, Y.; Takashima, Y.; Yamaguchi, H.; Harada, A. Preparation of cyclodextrin-based porous polymeric membrane by bulk polymerization of ethyl acrylate in the presence of cyclodextrin. *Polymer* **2019**, *17*, 208−213.
(35) Wondu, E.; Lule, Z. C.; Kim, J. Fabrication of high dielectric properties and high thermal conductivity polyurethane composites with CNT-covered $SrTiO_3$. *Polym. Test.* **2022**, *110*, No. 107576.
(36) Jayasinghe, G. D. T. M.; Jinadasa, B. K. K. K.; Pohl, P.; Abdelkarim, A. Critical review on microextraction techniques used in determination of histamine in food samples. *Discover Food* **2022**, *2*, 8.
(37) Elik, A.; Altunay, N.; Gürkan, R. Ultrasound-assisted low-density solvent-based dispersive liquid-liquid microextraction coupled to spectrophotometry for the determination of low levels of histamine in fish and meat products. *Food Anal. Methods* **2018**, *12*, 489−502.
(38) Papageorgiou, M.; Lambropoulou, D.; Morrison, C.; Klodzinska, E.; Namiesnik, J.; Plotka-Wasylka, J. Literature update of analytical methods for biogenic amines determination in food and beverages. *TrAC, Trends Anal. Chem.* **2018**, *98*, 128−142.
(39) Hasanzadeh, M.; Shadjou, N.; de la Guardia, M. Aptamer-based assay of biomoleculs: recent advances in electro-analytical approach. *TrAC, Trends Anal. Chem.* **2017**, *89*, 119−132.
(40) Wang, X.; Chen, Y.; Yu, R.; Wang, R.; Xu, Z. A sensitive biomimetic enzyme-linked immunoassay method based on Au@Pt@Au composite nanozyme label and molecularly imprinted biomimetic antibody for histamine detection. *Food Agric Immunol.* **2021**, *32*, 592−605.
(41) Mahnashi, M. H.; Mahmoud, A. M.; Alhazzani, K.; Alanzai, A. Z.; Algahtani, M. M.; Alaseem, A. M.; Alqahtani, Y. S. A.; El-Wekil, M. M. Enhanced molecular imprinted electrochemical sensing of

https://doi.org/10.1021/acsomega.3c00768
ACS Omega 2023, 8, 13352−13361

histamine based on signal reporting nanohybrid. *Microchem. J.* **2021**, *168*, No. 106439.
(42) Fan, Y.; Yu, R.; Chen, Y.; Sun, Y.; Waterhouse, G. I. N.; Xu, Z. A capillary electrophoresis method based on molecularly imprinted solid-phase extraction for selective and sensitive detection of histamine in foods. *Molecules* **2022**, *27*, 6987.
(43) Peng, X.; Chen, Y.; Gao, C.; Sun, Y.; Waterhouse, G. I. N.; Xu, Z. Development of an immunoassay method for the sensitive detection of histamine and tryptamine in foods based on a CuO@Au nanoenzyme lavel and molecularly imprinted biomimetic antibody. *Polymer* **2023**, *15*, 21.

https://doi.org/10.1021/acsomega.3c00768
ACS Omega 2023, 8, 13352−13361